Ramsey patterns for multiquantum transitions in fountain experiments

Douglas McColm

Physics Department, University of California at Davis, Davis, California 95616
and Chemical Sciences Division, Lawrence Berkeley National Laboratory, One Cyclotron Road, Berkeley, California 94720

Ramsey patterns for radio-frequency multiquantum transitions among Zeeman levels of the ground state of thallium, cesium, and francium have been calculated. The narrowing of these patterns observed earlier by Gould is predicted to occur only when both static electric and magnetic fields are present. [S1050-2947(96)04412-5]

INTRODUCTION

In preparing for a new generation of searches for an electron electric dipole moment, the new fountain technology on trapped atoms [1–3] is being considered. The most recently obtained limit on the electron electric dipole moment [4–6] did not use this technology.

Radio-frequency magnetic transitions among Zeeman levels of the ground state of a heavy atom are used in these searches. The method of separated oscillating fields due to Ramsey [7,8] appears to be a useful technique here for three reasons. First, it arises naturally in fountain experiments, since atoms traversing the radio-frequency region on the way up will traverse it again on the way down. Second, the technique generates very narrow resonance patterns, on the order of 1 Hz [9], since effects of magnetic- and electric-field inhomogeneities are very nearly eliminated. Thirdly, the technique reduces velocity-dependent systematic errors, because the average velocity of the atoms during the time between the two encounters with the radio-frequency field is zero.

The fact that resonance patterns from a single radio-frequency region associated with a multiquantum transition are narrower than those associated with single-quantum transitions was predicted by Salwen [10] and observed by Kusch [11]. Further theoretical work was done by Franzen and Alam [12] and by Phillips and Koh [13]. A corresponding narrowing using the Ramsey technique was observed by Gould [14].

This study was undertaken to predict the conditions under which narrowing occurred in Ramsey patterns associated with multiquantum transitions within the levels of a single hyperfine state. In the cesium $F=4$ levels for example, this narrowing effect would make the eight-quantum transition eight times narrower than the single-quantum transition, thereby increasing the precision by nearly an order of magnitude.

There is another advantage of multiquantum transitions for electric dipole moment searches. The direction of the moment, if it exists, is expected to lie along F_z, so that a multiquantum transition from M_F to $-M_F$ would completely reverse the orientation of the moment.

METHOD FOR CALCULATING THE TRANSITION PROBABILITY

The method of calculation used here is an extension of the technique used by Ramsey [7,8]; this extension allows both static electric and magnetic fields to be present, and also allows the total angular momentum F to be greater than $\frac{1}{2}$. Only one hyperfine state was used in this calculation, however. The static electric and magnetic fields were assumed to be parallel, along the z axis; the radio-frequency fields were taken to lie along the x axis.

The Hamiltonian defining the energy levels is

$$\mathcal{H} = \mathcal{H}_0 - \mathbf{p} \cdot \mathbf{E} - \boldsymbol{\mu} \cdot \mathbf{H}, \tag{1}$$

where $\mathcal{H}_0$ is the part of the Hamiltonian independent of the static fields $\mathbf{E}$ and $\mathbf{H}$. The energy levels associated with this Hamiltonian were calculated using the method of Angel and Sandars [15] (see the Appendix). For a geometry in which both $\mathbf{E}$ and $\mathbf{H}$ are along the z axis the result is

$$\mathcal{E} = \mathcal{E}_0 - \frac{1}{2} \alpha_s E_z^2 - \frac{1}{2} \alpha_t \frac{3M_F^2 - F(F+1)}{F(2F-1)} E_z^2 + g_F \mu_0 M_F H_z. \tag{2}$$

Here α_s and α_t are the scalar and tensor polarizabilities, respectively, and μ_0 is the Bohr magneton. Since the first two terms in this expression are independent of M_F, they were omitted in what follows since this paper is only concerned with low-frequency transitions among the energy levels associated with one particular F value in the ground state.

Standard time-dependent perturbation theory was employed, with a perturbation Hamiltonian,

$$\mathcal{H}' = -\boldsymbol{\mu} \cdot \mathbf{H}_{\mathrm{rf}} = g_F \mu_0 \mathbf{F} \cdot \mathbf{H}_{\mathrm{rf}}, \tag{3}$$

where

$$\mathbf{H}_{\mathrm{rf}} = H_{\mathrm{rf}}(\cos\omega t)\hat{\mathbf{x}} \tag{4}$$

and where μ_0 is the Bohr magneton.

The nonzero matrix elements of $\mathcal{H}'$ are

$$\langle M | \mathcal{H}' | M+1 \rangle = \frac{\hbar}{2} \gamma_M \cos\omega t, \tag{5}$$

$$\langle M | \mathcal{H}' | M-1 \rangle = \frac{\hbar}{2} \gamma_{-M} \cos\omega t, \tag{6}$$

where

$$\gamma_M = \frac{g_F \mu_0 H_{\mathrm{rf}}}{\hbar} \sqrt{(F-M)(F+M+1)} \qquad (7)$$

and where M is an abbreviation for M_F.

In writing the equations of the perturbation theory, the quantity $\cos \omega t$ in Eq. (4) is normally broken into two terms, $\frac{1}{2} e^{i\omega t}$ and $\frac{1}{2} e^{-i\omega t}$, only one of which will be resonant. One discards the nonresonant term, because then the time dependence is easily separated from the equations of the perturbation theory. However, the resonant and nonresonant terms can exchange roles at the level crossings, which occur because both static electric and magnetic fields are present. For example, in the $F=1$ hyperfine levels of the thallium ground state, the terms $\exp\{i[(\mathcal{E}_0 - \mathcal{E}_{-1})/\hbar - \omega]t\}$ and $\exp\{i[(\mathcal{E}_0 - \mathcal{E}_{-1})/\hbar + \omega]t\}$ occur. The first will be resonant when $\mathcal{E}_0 > \mathcal{E}_{-1}$ and the second when $\mathcal{E}_0 < \mathcal{E}_{-1}$. This reversal occurs at the level crossing (see Fig. 2). In order to unambiguously select the resonant term, the quantities η_M and Ω_M are introduced:

$$\eta_M = \begin{cases} \dfrac{\mathcal{E}_{M+1} - \mathcal{E}_M}{|\mathcal{E}_{M+1} - \mathcal{E}_M|}, & \mathcal{E}_{M+1} \neq \mathcal{E}_M \qquad (8) \\ 1, & \mathcal{E}_{M+1} = \mathcal{E}_M \qquad (9) \end{cases}$$

$$\Omega_{M+1} = \sum_{M'=-F}^{M} \eta_{M'}, \qquad M \geq -F \qquad (10)$$

$$\Omega_{-F} = 0. \qquad (11)$$

Then, writing the wave function in the usual form,

$$\psi = \sum_M |M\rangle B_M(t) e^{-i\mathcal{E}_M t/\hbar}, \qquad (12)$$

the equations of the perturbation theory are

$$i\frac{dB_F}{dt} = \frac{\gamma_{-F}}{4} B_{F-1} e^{-i(\eta_{F-1}\omega - \omega_{F,F-1})t}, \qquad (13)$$

$$i\frac{dB_M}{dt} = \frac{\gamma_M}{4} B_{M+1} e^{i(\eta_M \omega - \omega_{M+1,M})t}$$
$$+ \frac{\gamma_{-M}}{4} B_{M-1} e^{-i(\eta_{M-1}\omega - \omega_{M,M-1})t},$$
$$-F < M < F \quad (14)$$

$$i\frac{dB_{-F}}{dt} = \frac{\gamma_{-F}}{4} B_{-F+1} e^{i(\eta_{-F}\omega - \omega_{-F+1,-F})t}, \qquad (15)$$

where

$$\omega_{M,M'} = (\mathcal{E}_M - \mathcal{E}_{M'})/\hbar. \qquad (16)$$

The time dependence in the equation above can be removed by letting B_M have the following form:

$$B_M = b_M e^{i[(\omega_{M,-F} - \Omega_M \omega) - \beta]t}. \qquad (17)$$

Here the b_M are time independent.

The equations for the b_M are

$$[(\omega_{F,-F} - \Omega_F \omega) - \beta]b_F + \frac{\gamma_{-F}}{4} b_{F-1} = 0, \qquad (18)$$

$$\frac{\gamma_M}{4} b_{M+1} + [(\omega_{M,-F} - \Omega_M \omega) - \beta]b_M + \frac{\gamma_{-M}}{4} b_{M-1} = 0,$$
$$-F < M < F \quad (19)$$

$$\frac{\gamma_{-F}}{4} b_{-F+1} - \beta b_{-F} = 0, \qquad (20)$$

and constitute an eigenvalue problem for eigenvalues β and eigenvectors b_M.

A standard computer package was used to calculate the eigenvalues and eigenvectors. There are $2F+1$ of these, which are called β_k and $b_M^{(k)}$, respectively, the index k distinguishing the various eigenvalues: $-F \geq k \geq F$. Thus the $B_M(t)$ for the atoms leaving the rf region the first time at time t are equal to

$$B_M = \sum_k c_k b_M^{(k)} e^{i[(\omega_{M,-F} - \Omega_M \omega) - \beta_k]t}, \qquad (21)$$

where the coefficients c_k are chosen so that the boundary condition, the atom is initially in the state M_0, is satisfied. That is,

$$\sum_k c_k b_M^{(k)} = \delta_{M,M_0}. \qquad (22)$$

This is an inhomogeneous linear set of equations in the c_k, and so another standard package was used in the computer calculation.

As the atoms move in the fountain up and down, outside of the rf region, the quantities B_M do not change. If the atoms reenter the rf region at time T, then

$$B_M(T) = B_M(t) \qquad (23)$$

is the boundary condition defining coefficients c_k' that describe B_M in the rf region the second time. This is also an inhomogeneous set of linear equations, and the same standard package was used in the computer calculation.

Finally, when the atoms exit the apparatus at time $T+t$, the B_M have the value

$$B_M(T+t) = \sum_k c_k' b_M^{(k)} e^{i[(\omega_{M,-F} - \Omega_M \omega) - \beta_k](T+t)} \qquad (24)$$

and the transition probability is of course just $|B_M(T+t)|^2$.

The results reported below apply to the center of the Ramsey pattern. For a multiple-quantum transition, the center frequency is not the the difference between the energies of the initial and final states divided by the number of the quanta. For example, the $M_F = F$ and $M_F = -F$ levels are degenerate in a static electric field (with no magnetic field present) and a multiple-quantum transition between these levels does not occur at zero frequency but rather at the average frequency of the single-quantum transitions between these levels. This criterion for the central frequency also works when only a
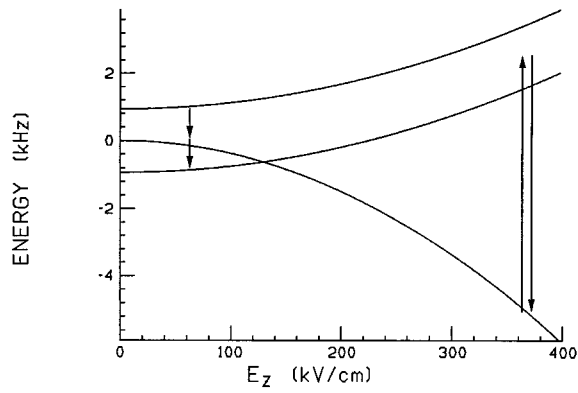
FIG. 1. $F=1$ hyperfine levels of the ground state of thallium as a function of static electric field. The static magnetic field present is 0.002 G. The level crossing in the figure is in fact an "avoided" crossing; in the presence of a nonzero H_x, the crossing does not occur. The two-quantum $M_F=1 \rightarrow M_F=-1$ transitions at low and high electric fields are indicated by the arrows.

static magnetic field is present, and was employed as the definition of the central frequency in all the cases between, where both electric and magnetic fields are present. The energies associated with these frequencies are shown by the arrows in Figs. 1, 3, and 7. When the electric field is small the arrows connect exactly to the $M_F=F$ and $M_F=-F$ levels, with the levels in between being somewhat out of resonance. When the electric field is large and the magnetic field is nonzero, then the arrows connect exactly to the $M_F=0$ level, with the other levels being somewhat out of resonance. (And when the magnetic field is zero, then the arrows connect exactly to the $M_F=F$ and $M_F=-F$ levels as well as to the $M_F=0$ levels.)

The results reported below assumed times T and t of 0.3 and 0.005 s, respectively.

RESULTS FOR THALLIUM $F=1$ GROUND-STATE LEVELS

The energies of the $J=\frac{1}{2}$, $I=\frac{1}{2}$, $F=1$ thallium ground-state levels in the presence of both electric and magnetic fields are shown in Fig. 1. The two-quantum transitions between the $M_F=1$ and -1 transitions in the low-electric-field and high-electric-field cases are indicated by the arrows. The level crossing shown is an "avoided" crossing; in the presence of a nonzero H_x magnetic-field component, it does not occur.

The results of the calculations are shown in Fig. 2. In the region labeled D, the Ramsey oscillations are predicted to show the behavior found by Gould, while in region S, the Ramsey patterns for the one-quantum and two-quantum transitions should have the same spacing. The boundary between these two regions is somewhat diffuse and fills the space between the dashed lines.

Thus, when run at the conditions that were used by Gould [14] (namely, $H_z=1$ G and $E_z=240$ kV/cm), the program gave the same result that he found, namely, the oscillations of the two-quantum Ramsey pattern were twice as closely spaced as those of the one-quantum transition. However, when either the static magnetic or static electric fields were set to zero, the calculations predicted that this effect should be absent, that the Ramsey patterns for the one-quantum and
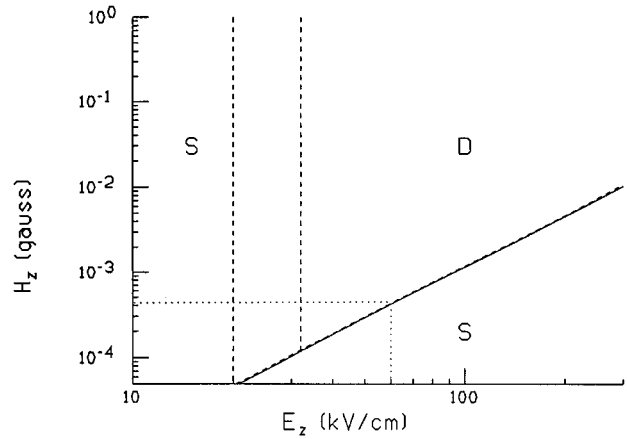

FIG. 2. Schematic of the Ramsey patterns in the $F=1$ thallium ground state. In the S region, the one-quantum and two-quantum Ramsey patterns are predicted to have the same spacing; in region D, the two-quantum transition is predicted to have a Ramsey pattern twice as closely spaced as the one-quantum transition. The dots enclose the region where the period of the rf oscillations is greater than the time t the atoms spend experiencing the rf field, so that the atoms experience less than one cycle of the rf during their transit of either of the rf regions.

two-quantum transitions should have the same spacing. This statement should be independent of whether the atoms have a broad velocity distribution, such as was true in Gould's experiment, or a negligible one, as in contemporary fountain experiments.

In these calculations, the rf amplitude was chosen in each case to have the value that optimized the overall transition probability at the resonant frequency. Figure 2 is roughly the same, however, if the rf amplitude is held constant; in this case the vertical boundary between the D and S regions is shifted somewhat, depending on the value chosen for the rf amplitude.

The values of α_t and g_F employed were $\alpha_t=-3.74\times10^{-8}$ Hz/(V/cm) [14], $g_F=0.3342$.

Because the relevant levels in thallium have a small value of F, namely, $F=1$, a calculation by hand was attempted, since this was a very surprising result.

When the static electric field is zero, the levels are equally spaced due to the magnetic field, and the eigenvalues β can be expressed in terms of two parameters: $\Gamma=g_F\mu_0H_{rf}/2\hbar$, the rf power parameter, and $\eta=\frac{1}{2}(\omega_{1,0}+\omega_{0,-1})-\omega$, the frequency deviation parameter. The latter is the distance in frequency units from the center of the resonance pattern. When $\eta\ll\Gamma$ then the three eigenvalues β are

$$\beta=-\Gamma+\eta, \quad \eta, \quad \Gamma+\eta. \quad (25)$$

Then, if $t\ll T$, the transition probability at optimum rf power between the $M_F=1$ and -1 levels is

$$|B_{-1}(T+t)|^2=\cos^4\eta T/2 \quad (26)$$

so that the spacing between Ramsey fringes is $\Delta\eta=2\pi/T$.

When the static electric field is nonzero, but not so large that the level crossing is reached (see Fig. 1), the parameter $\zeta=(\omega_{0,-1}-\frac{1}{2}\omega_{1,-1})/2\Gamma$ is introduced as a measure of how much the equal spacing of the energy levels has been dis-

torted by the presence of the static electric field. In fact, ζ is directly proportional to the square of the electric field:

$$\zeta = \frac{3\alpha_t E_z^2}{2g_F \mu_0 H_{\text{rf}}}. \qquad (27)$$

When both $\zeta \ll 1$ and $\eta \ll \Gamma$, the eigenvalues β are

$$\beta = -\Gamma(1 - \zeta + \tfrac{1}{2}\zeta^2) + \eta, \quad \eta, \quad \Gamma(1 + \zeta + \tfrac{1}{2}\zeta^2) + \eta. \qquad (28)$$

To lowest order in ζ the transition probability is

$$|B_{-1}(T+t)|^2 = \cos^4 \frac{\eta T}{2} - \frac{\zeta^2}{2} \sin^2 \eta T \qquad (29)$$

under the limitations $\zeta \ll 1$, $\eta \ll \Gamma$, $t \ll T$. Also, corrections to the optimum power condition due to the presence of ζ were neglected.

Thus as ζ increases, more closely spaced Ramsey fringes are predicted, arising from the presence of the $\sin^2 \eta T$ term. Of course, for large ζ, terms higher order in ζ will participate so this prediction is necessarily quite rough. But one might expect the more closely spaced Ramsey fringes to arise for a ζ value somewhere between 0 and 1. Now $\zeta = \tfrac{1}{2}$ when E_z is about 25 kV/cm, so the presence of a D region would be explained if its onset occurred in the neighborhood of this value. The computer calculation predicted the onset of the D region between 20 and 30 kV/cm, which is consistent with this requirement.

The onset of this effect should not be abrupt, but since it depends on E_z^4, it should occur over a rather narrow electric-field region. Furthermore, the onset should be independent of the value of the static magnetic field since ζ is independent of H_z. These conclusions agree with the results of the computer calculation.

The solid line in Fig. 2 indicates the position of the level crossing in this state of thallium. The discussion above applies to the region above this line. But below this line, all the two-quantum Ramsey patterns had the same spacing as the single-quantum ones. The boundary between S and D regions directly follows this line. This boundary is found both using the central frequency defined above and also using the frequency $\omega_{1,-1}/2$. No frequency was found which gave a D region below this line.

This is also surprising behavior. Of course at the level crossing, some of the resonant and nonresonant terms described in the preceding section change roles so that $\Omega_1 = 2$ above the dashed line and $\Omega_1 = 0$ below it. Again a hand calculation was done. The frequency deviation parameter was $\eta = \omega - \tfrac{1}{2}(\omega_{1,0} + \omega_{-1,0})$. And since the $M_F = 1$ and -1 levels are degenerate when the static magnetic field is zero, the distortion parameter was $\zeta = \omega_{1,-1}/2\Gamma$. The eigenvalues β had the values

$$-\Gamma(1 - \zeta + \tfrac{1}{2}\zeta^2) - \frac{\eta}{2}, \quad \Gamma\zeta, \quad \Gamma(1 + \zeta + \tfrac{1}{2}\zeta^2) - \frac{\eta}{2} \qquad (30)$$

provided both $\zeta \ll 1$ and $\eta \ll \Gamma$. The η dependence contains a factor of $\tfrac{1}{2}$, which is absent in Eq. (28), suggesting that the

spacing of the Ramsey fringes should be fundamentally different in this region that in the previous one.

The hand calculation was carried out to lowest order in ζ, with the assumptions $\zeta \ll 1$, $\eta \ll \Gamma$, and $t \ll T$ as before, with the result that

$$|B_{-1}(T+t)|^2 = (1 - 2\zeta^2)\cos^2 \frac{\eta T}{2} \qquad (31)$$

provided again that the corrections to the optimum rf power condition due to nonzero ζ were neglected. This result shows that to order ζ^2, no change in the spacing of the Ramsey fringes was found in this region, in agreement with the computer calculations.

Thus these hand calculations showed that the basic features of Fig. 2 in the restricted regions $\zeta \ll 1$, $\eta \ll \Gamma$, and $t \ll T$ could be explained: The change in spacing of the Ramsey fringes in the upper region of Fig. 2 is due to the unequal separations between the energy levels because of the presence of the electric field. Then, because of the reversal of the resonant and nonresonant factors in the perturbation theory, no such change occurs in the lower region of Fig. 2.

RESULTS FOR CESIUM $F = 4$ GROUND-STATE LEVELS

The energies of the $J = \tfrac{1}{2}$, $I = \tfrac{7}{2}$, $F = 4$ levels of the cesium ground state are shown in Figs. 3(a) and 3(b). Arrows indicate the eight-quantum transition $M_F = 4$ to -4, both in low and high static electric field. There are many level crossings, all of which are "avoided" crossings.

The results of the computer calculations for these cesium transitions are similar to those for thallium. (See Fig. 4.) A region S is present where the Ramsey patterns for the one-quantum and eight-quantum transitions should have the same spacing. This region includes both the axes. The eight-quantum pattern was predicted not to be sinusoidal, however, but should have markedly narrowed central peaks, as shown in Fig. 5(a).

Then there is a central region, M, where the eight-quantum transition is predicted to have a much more closely spaced Ramsey pattern than does region S. The boundary between these two regions is more diffuse than in the thallium case.

The level crossings which occur at the lowest values of electric field [see Fig. 3(a)] lie very close to the curved boundary in Fig. 4, but without a hand calculation, it is not possible to determine which of these crossings plays a vital role in defining the boundary. Because of the high value of F and the large number of level crossings, a hand calculation would be very difficult and was not attempted.

The possibility of using region M for high-precision experiments involves the following difficulty: In region S the dependence of the transition probability on the radio-frequency amplitude showed a series of broad peaks which would be straightforward to employ in experiments, while in region M the dependence consisted of many rapid, irregular variations that would be much more difficult to use. (See Fig. 6.)

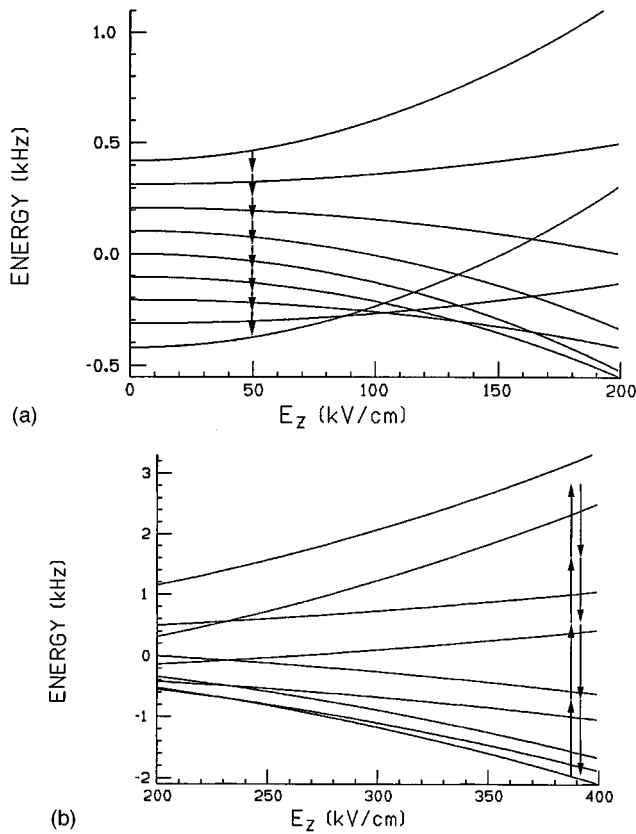The $F = 3$ levels of the cesium ground state behave similarly.

FIG. 3. $F=4$ hyperfine levels of the ground state of cesium as a function of static electric field. The static magnetic field present is 0.0003 G. The level crossings in the figure are in fact "avoided" crossings; in the presence of a nonzero H_x, the crossings do not occur. The eight-quantum $M_F=4 \rightarrow M_F=-4$ transitions at low (a) and high (b) electric fields are indicated by the arrows.
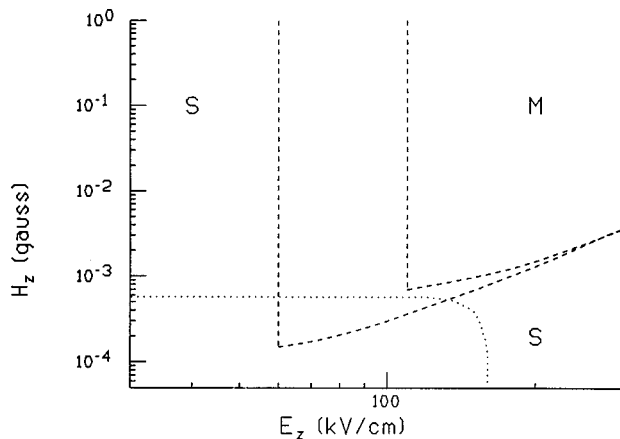

FIG. 4. Schematic of the Ramsey patterns in the $F=4$ cesium ground state. In the S region, the one-quantum and eight-quantum Ramsey patterns are predicted to have the same spacing; in region M, the eight-quantum transition is predicted to have a Ramsey pattern eight times as closely spaced as the one-quantum transition. The dots enclose the region where the period of the rf oscillations is greater than the time t the atoms spend experiencing the rf field, so that the atoms experience less than one cycle of the rf during their transit of either of the rf regions.
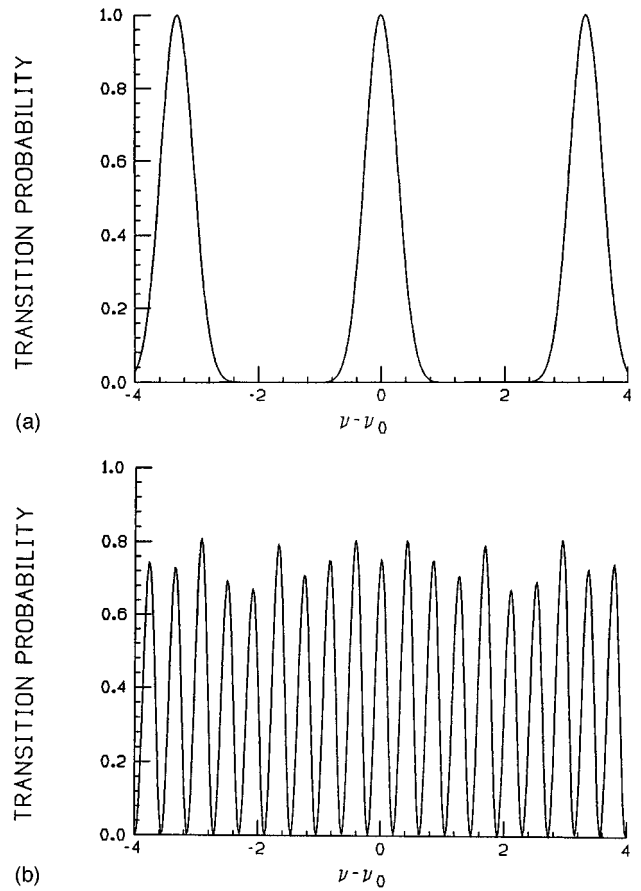

FIG. 5. Predicted Ramsey patterns in the $F=4$ hyperfine levels of the cesium ground state. (a) The eight-quantum Ramsey pattern in region S, for $H_z=1$ G and $E_z=0$. (b) The eight-quantum Ramsey pattern in region M, for $H_z=1$ G and $E_z=300$ kV/cm.

The values of α_t and g_F employed were $\alpha_t = -0.3659 \times 10^{-7}$ Hz/(V/cm) [14], $g_F=0.2504$.

RESULTS FOR FRANCIUM $F=3$ GROUND-STATE LEVELS

The energies of the $J=\frac{1}{2}$, $I=\frac{5}{2}$, $F=3$ levels of the francium ground state are shown in Figs. 7(a) and 7(b). Arrows indicate the six-quantum transition $M_F=3$ to -3, both in low and high static electric field. There are many level crossings, all of which are "avoided" crossings.

The tensor polarizability of the $F=3$ ground-state levels in francium has not been measured, so an estimate was made using the cesium tensor polarizability value. This estimate is shown in Fig. 8. The S and M regions are defined just as in the cesium $F=4$ case.

The g_F value employed was 0.3336.

CONCLUSION

The multiquantum transition $M_F=F$ to $-F$ is useful in experiments searching for an electron electric dipole moment since in such a transition the electric dipole moment of the atom, if it existed, would completely reverse in direction, giving rise to the maximum possible effect on the energy.

The motional magnetic field $\mathbf{v} \times \mathbf{E}/c$ arising from the motion of the atoms through the electric field is a major source
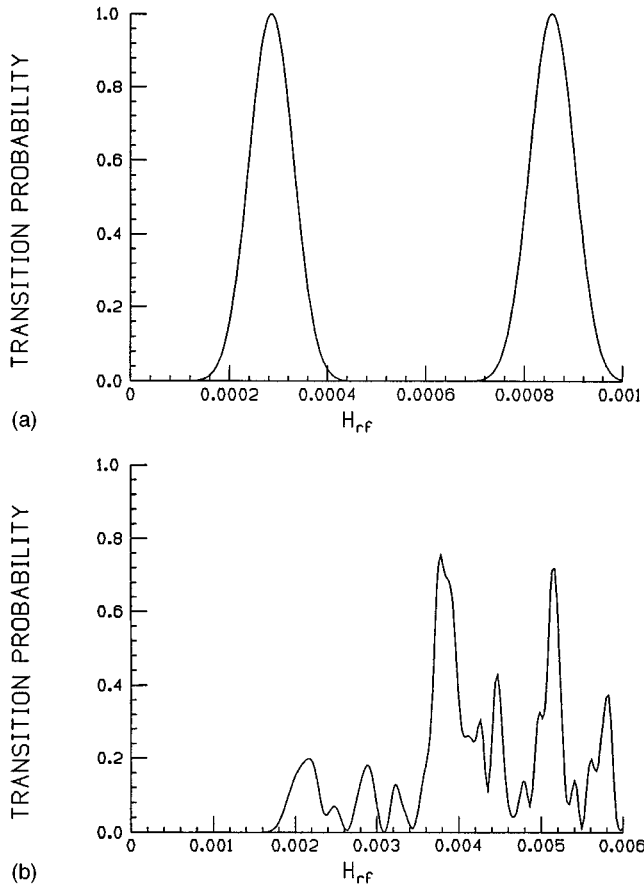
(a)

(b)

FIG. 6. Dependence of the transition probability on rf amplitude for Ramsey patterns in the $F=4$ hyperfine levels of the cesium ground state: (a) for the eight-quantum Ramsey pattern in region S, for $H_z=1$ G and $E_z=0$; (b) for the eight-quantum Ramsey pattern in region M, for $H_z=1$ G and $E_z=300$ kV/cm.

of systematic errors in electric dipole moment searches, because its effects are similar to those associated with an atomic electric dipole moment. In a representation where the quantization direction is taken to be along the electric field this term would not be diagonal and hence would not directly influence the energy, a desirable state of affairs. To give an observable effect the $\mathbf{v}\times\mathbf{E}/c$ term would need to combine with some other off-diagonal effect, such as an interaction with an x or y component of the static magnetic field; such a combined electric-magnetic perturbation was discussed by Player and Sandars [16]. In order to rule out such terms, one would like to have the static magnetic field either zero or at least parallel to the static electric field.

Thus one might plan to have the magnetic field in an electron electric dipole moment search as small as possible, but then the closely spaced Ramsey fringes giving the most sensitivity would not be observed. As seen in Figs. 1, 4, and 8, these only occur at nonzero magnetic field. But if the magnetic field is nonzero, then it must be very accurately parallel to the electric field if systematic $\mathbf{v}\times\mathbf{E}/c$ errors are to be avoided.
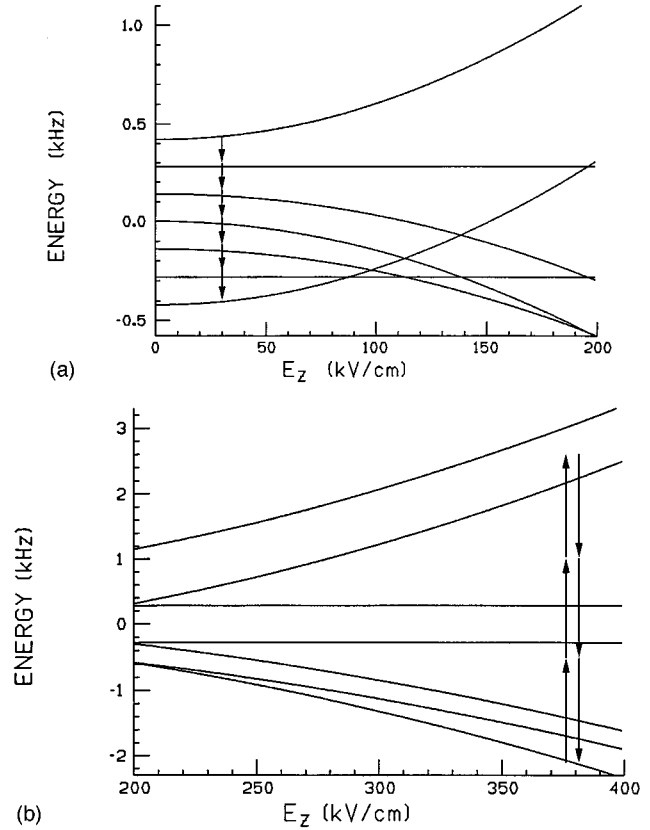
(a)

(b)

FIG. 7. $F=3$ hyperfine levels of the ground state of francium as a function of static electric field. The static magnetic field present is 0.0003 G. The level crossings in the figure are in fact ''avoided'' crossings; in the presence of a nonzero H_x, the crossings do not occur. The six-quantum $M_F=3\rightarrow M_F=-3$ transitions at low (a) and high (b) electric fields are indicated by the arrows.
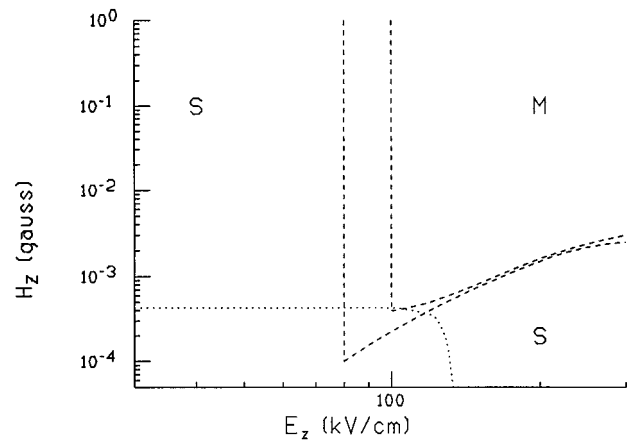

FIG. 8. Schematic of the Ramsey patterns in the $F=3$ hyperfine levels of the francium ground state. In the S region, the one-quantum and six-quantum transitions have the same spacing; in region M, the six-quantum transition is predicted to have a Ramsey pattern six times as closely spaced as the one-quantum transition. The dots enclose the region where the period of the rf oscillations is greater than the time t the atoms spend experiencing the rf field, so that the atoms experience less than one cycle of the rf during their transit of either of the rf regions.

APPENDIX

The method of Angel and Sandars [15] was used to evaluate the energy of the $-\mathbf{p}\cdot\mathbf{E}$ Hamiltonian. It relies on second-order perturbation theory, the first-order term being zero on parity grounds

$$\mathcal{E}=\mathcal{E}_0+\sum_{n\neq 0}\frac{\langle 0|\mathbf{p}\cdot\mathbf{E}|n\rangle\langle n|\mathbf{p}\cdot\mathbf{E}|0\rangle}{\mathcal{E}_0-\mathcal{E}_n}. \tag{A1}$$

With the definition

$$\lambda=\sum_{n\neq 0}\frac{|n\rangle\langle n|}{\mathcal{E}_0-\mathcal{E}_n} \tag{A2}$$

the energy becomes

$$\mathcal{E}=\mathcal{E}_0+\langle 0|(\mathbf{p}\cdot\mathbf{E})\lambda(\mathbf{p}\cdot\mathbf{E})|0\rangle. \tag{A3}$$

This expression is recoupled using the spherical tensor identity,

$$[A^{(k_1)}\cdot B^{(k_1)}][C^{(k_2)}\cdot D^{(k_2)}]$$

$$=\sum_K (-1)^{k_1+k_2+K}\{A^{(k_1)}C^{(k_2)}\}^{(K)}\cdot\{B^{(k_1)}D^{(k_2)}\}^{(K)}, \tag{A4}$$

with the result

$$(\mathbf{p}\cdot\mathbf{E})\lambda(\mathbf{p}\cdot\mathbf{E})=\{\mathbf{p}\lambda\mathbf{p}\}^{(0)}\cdot\{\mathbf{E}\mathbf{E}\}^{(0)}+\{\mathbf{p}\lambda\mathbf{p}\}^{(2)}\cdot\{\mathbf{E}\mathbf{E}\}^{(2)}. \tag{A5}$$

The scalar and tensor polarizabilities α_s and α_t are defined in terms of these operators. In the case that the electric field is along the z axis, these definitions are

$$\langle F,F|\{\mathbf{p}\lambda\mathbf{p}\}^{(0)}\cdot\{\mathbf{E}\mathbf{E}\}^{(0)}|F,F\rangle=-\tfrac{1}{2}\alpha_s E_z^2, \tag{A6}$$

$$\langle F,F|\{\mathbf{p}\lambda\mathbf{p}\}^{(2)}\cdot\{\mathbf{E}\mathbf{E}\}^{(2)}|F,F\rangle=-\tfrac{1}{2}\alpha_t E_z^2, \tag{A7}$$

where $|F,F\rangle$ is $|F,M_F\rangle$ with $M_F=F$. In terms of reduced matrix elements, α_s and α_t turn out to be

$$\alpha_s=\frac{2}{\sqrt{3}}\frac{(F\|\{\mathbf{p}\lambda\mathbf{p}\}^{(0)}\|F)}{\sqrt{2F+1}}, \tag{A8}$$

$$\alpha_t=-\frac{4}{\sqrt{6}}\left(\frac{2F(2F-1)}{(2F+3)(2F+2)(2F+1)}\right)^{1/2}(F\|\{\mathbf{p}\lambda\mathbf{p}\}^{(2)}\|F). \tag{A9}$$

Then the expression for the energy $\mathcal{E}$ given above can be directly evaluated using the Wigner-Eckhart theorem, giving the result quoted in the second section of this paper.

---

[1] M. A. Kasevich, E. Riis, and S. Chu, Phys. Rev. Lett. **63**, 612 (1989).

[2] A. Clairon, Ph. Laurent, A. Nadir, G. Santarelli, M. Drewsen, D. Grison, B. Lounis, and C. Salomon, Proc. SPIE **1837**, 306 (1992).

[3] H. Metcalf and P. van der Straten, Phys. Rep. **244**, 203 (1994).

[4] K. Abdullah, C. Carlberg, E. D. Commins, H. Gould, and S. B. Ross, Phys. Rev. Lett. **65**, 2347 (1990).

[5] E. D. Commins, S. B. Ross, D. DeMille, and B. C. Regan, Phys. Rev. A **50**, 2960 (1994).

[6] S. A. Murthy, D. Krause, Jr., Z. L. Li, and L. R. Hunter, Phys. Rev. Lett. **63**, 965 (1989).

[7] N. F. Ramsey, Phys. Rev. **78**, 695 (1950).

[8] N. F. Ramsey, Rev. Mod. Phys. **62**, 541 (1990).

[9] A. Clairon, C. Salomon, S. Guellati, and W. D. Phillips, Europhys. Lett. **16**, 165 (1991).

[10] H. Salwen, Phys. Rev. **101**, 623 (1956).

[11] P. Kusch, Phys. Rev. **101**, 627 (1956).

[12] W. Franzen and M. Alam, Phys. Rev. **133**, A460 (1964).

[13] E. A. Phillips and T. K. Koh, Phys. Rev. A **2**, 263 (1970).

[14] H. Gould, Phys. Rev. A **14**, 922 (1976).

[15] J. R. P. Angel and P. G. H. Sandars, Proc. R. Soc. London Ser. A **305**, 125 (1968).

[16] M. A. Player and P. G. H. Sandars, J. Phys. B **3**, 1620 (1970).